LANGMUIR
Cite This: Langmuir 2019, 35, 8436−8444
Article
pubs.acs.org/Langmuir

Understanding How Membrane Surface Charge Influences Lipid Bicelle Adsorption onto Oxide Surfaces

Tun Naw Sut,[†] Joshua A. Jackman,[‡] and Nam-Joon Cho*[,†,§]

[†]School of Materials Science and Engineering, Nanyang Technological University, 50 Nanyang Avenue 639798, Singapore
[‡]School of Chemical Engineering, Sungkyunkwan University, Suwon 16419, Republic of Korea
[§]School of Chemical and Biomedical Engineering, Nanyang Technological University, 62 Nanyang Drive 637459, Singapore

Downloaded by NANYANG TECHNOLOGICAL UNIV at 02:06:57:926 on July 02, 2019
from https://pubs.acs.org/doi/10.1021/acs.langmuir.9b00570.

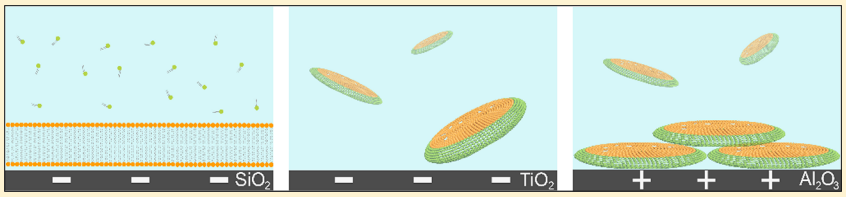

ABSTRACT: The adsorption of two-dimensional bicellar disks onto solid supports is an emerging fabrication technique to form supported lipid bilayers (SLBs) that is efficient and requires minimal sample preparation. To date, nearly all relevant studies have focused on zwitterionic lipid compositions and silica-based surfaces, and extending the scope of investigation to other lipid compositions and surfaces would improve our understanding of application possibilities and underpinning formation processes. Herein, using the quartz crystal microbalance-dissipation technique, we systematically investigated the adsorption of charged lipid bicelles onto silicon dioxide, titanium oxide, and aluminum oxide surfaces. Depending on the lipid composition and substrate, we observed different adsorption pathways, including (i) SLB formation via one- or two-step adsorption kinetics, (ii) monotonic adsorption without SLB formation, and (iii) negligible adsorption. On each substrate, SLB formation could be achieved with particular lipid compositions, whereas the trend in adsorption pathways varied according to the substrate and could be controlled by adjusting the bicelle−substrate interaction strength. To rationalize these findings, we discuss how electrostatic and hydration forces affect bicelle−substrate interactions on different oxide surfaces. Collectively, our findings demonstrate the broad utility of lipid bicelles for SLB formation while revealing physicochemical insights into the role of interfacial forces in controlling bicelle adsorption pathways.

INTRODUCTION

Achieving control over the self-assembly pathways by which phospholipid molecules adsorb onto a solid support is an important goal of nanoarchitectonic-based fabrication strategies[1,2] and can lead to improved biomimetic membrane platforms for various scientific and biotechnology applications.[3−5] In this respect, lipid bicelles are one of the most fascinating biomacromolecular assemblies, classically viewed as a two-dimensional disk-like lipid nanostructure that is composed of long-chain and short-chain phospholipids.[6,7] The precise structural organization of a bicelle in solution depends on numerous factors such as the total lipid concentration, ratio of long-chain to short-chain phospholipids ("q-ratio"), and environmental conditions, while preparation steps are straightforward and entail lipid hydration followed by a few rounds of freeze−thaw-vortexing.[8−11] Solution-phase bicelles first gained attention as a suitable lipid environment for reconstituting and studying transmembrane proteins in the structural biology field,[12,13] and recent findings have pointed to the practical utility of depositing bicellar mixtures on solid surfaces to fabricate supported lipid bilayers (SLBs).[14,15]

Zeineldin et al. first demonstrated that zwitterionic lipid bicelles can be employed to fabricate SLBs on flat and nanotextured, oxidized silicon surfaces.[16] Tabaei et al. also showed that bicelles could form fluidic SLBs on silicon dioxide surfaces, and introduced nucleic acid−based tethers to form stacks of multiple bicelle layers.[17] In that study, the inclusion of a positively charged detergent in the bicellar mixture was noted to significantly enhance bicelle adsorption. To shed light on the underlying mechanisms of bicelle-mediated SLB formation, Morigaki et al. conducted a systematic investigation examining how the q-ratio affects SLB formation on silicon dioxide surfaces, identifying the short-chain phospholipids can act as detergents that not only catalyze SLB formation but also disrupt the structure of fabricated SLBs.[18] Hence, it was suggested to select experimental conditions whereby the short-chain phospholipid concentration is below its critical micelle concentration.

Building on these studies, Kolahdouzan et al. further investigated how the interplay of total lipid concentration and q-ratio along with processing conditions affect bicelle-mediated SLB formation on silicon dioxide surfaces.[19] The findings revealed that bicelle-mediated SLB formation quality is optimal when using low lipid concentrations (∼0.02 mg/mL

Received: February 26, 2019
Revised: April 30, 2019
Published: May 29, 2019

ACS Publications © 2019 American Chemical Society

DOI: 10.1021/acs.langmuir.9b00570
Langmuir 2019, 35, 8436−8444

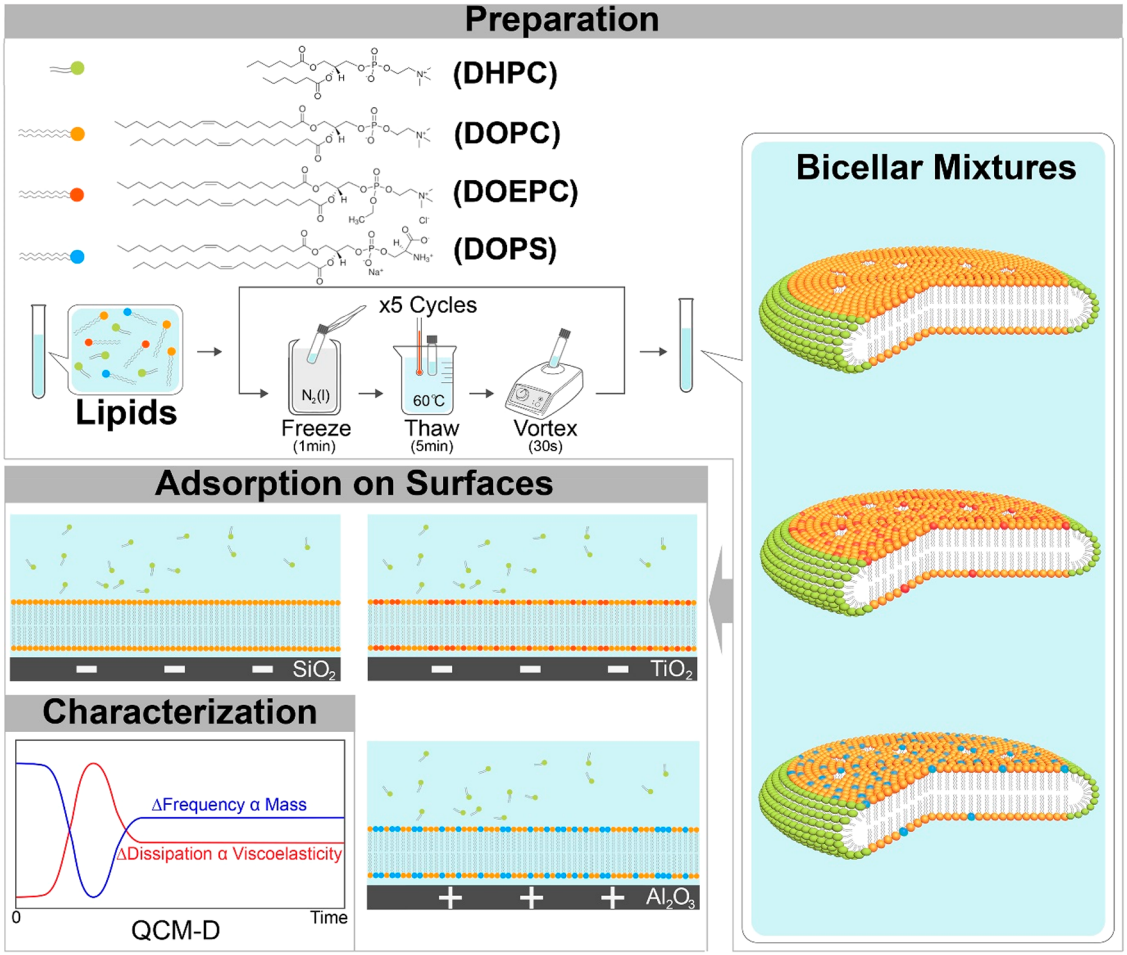

Figure 1. Overview of experimental framework. Zwitterionic lipid bicelles were composed of long-chain DOPC lipids and short-chain DHPC lipids. Charged lipid bicelles were prepared by mixing long-chain zwitterionic DOPC lipids with varying amounts (0–75 mol %, in 25 mol % increments) of long-chain, positively charged DOEPC lipids or negatively charged DOPS lipids, whereas the DHPC lipid fraction was kept constant. The total lipid concentration was fixed in all experiments. Lipid bicelle adsorption was tracked by QCM-D measurements. The illustrations are not drawn to scale.

or lower long-chain phospholipid concentration), which are far below the lipid concentrations reported in previous bicelle studies (typically ~0.2 mg/mL or greater long-chain phospholipid concentration). Important similarities and differences between bicelle-mediated and conventional vesicle-mediated SLB formation were also noted. While both types of lipid nanostructures rupture after a critical surface coverage of adsorbed bicelles or vesicles is reached to form silicon dioxide-supported SLBs, adsorbed bicelles undergo greater deformation than adsorbed vesicles, efficiently form SLBs at lower total lipid concentrations, and require a simpler preparation protocol. There are also mechanistic differences because the area of an SLB patch that is formed by the rupture of an adsorbed vesicle is larger than the vesicle–substrate contact area,[20] whereas the patch area that is formed by the rupture of an adsorbed bicelle is expected to be similar to the bicelle–substrate contact area. For all these reasons, there is broad potential for exploring bicelle-mediated SLB formation as a robust fabrication strategy and successful SLB formation based on covalent tethering of oxyamine-functionalized bicelles to polymeric surfaces has also been reported.[21] At the same time, due consideration of various experimental factors is warranted, and Yamada et al. recently showed that adsorbed bicelles align parallel in a stable configuration on a silicon dioxide surface, whereas amine-functionalized silicon dioxide surfaces were not conducive to supporting stable assemblies of adsorbed bicelles.[22] In light of these findings, it is important to systematically investigate how factors such as membrane surface charge and substrate type affect bicelle adsorption and SLB formation efficiency on different solid supports.

Herein, the objective of this study was to investigate how bicelle surface charge influences the bicelle adsorption process and subsequent SLB formation efficiency on three different oxide surfaces: silicon dioxide, titanium oxide, and aluminum oxide (Figure 1). While previous bicelle-mediated SLB formation studies focused on silica-based surfaces, there is broad interest in developing strategies to form SLBs on titanium oxide and aluminum oxide surfaces, especially due to the challenges of using the vesicle-based SLB formation method on these surfaces and the distinct material properties of the three surfaces [see recent examples of alternative techniques such as the solvent-assisted lipid bilayer (SALB) method[23,24] as well]. Likewise, the previous studies mainly dealt with zwitterionic lipid compositions and controlling bicelle surface charge—in our case by adjusting the molar fractions of zwitterionic 1,2-dioleoyl-*sn*-glycero-3-phosphocholine (DOPC) and 1,2-dioleoyl-*sn*-glycero-3-ethylphosphocholine (DOEPC) or 1,2-dioleoyl-*sn*-glycero-3-phospho-L-serine

DOI: 10.1021/acs.langmuir.9b00570
Langmuir 2019, 35, 8436–8444

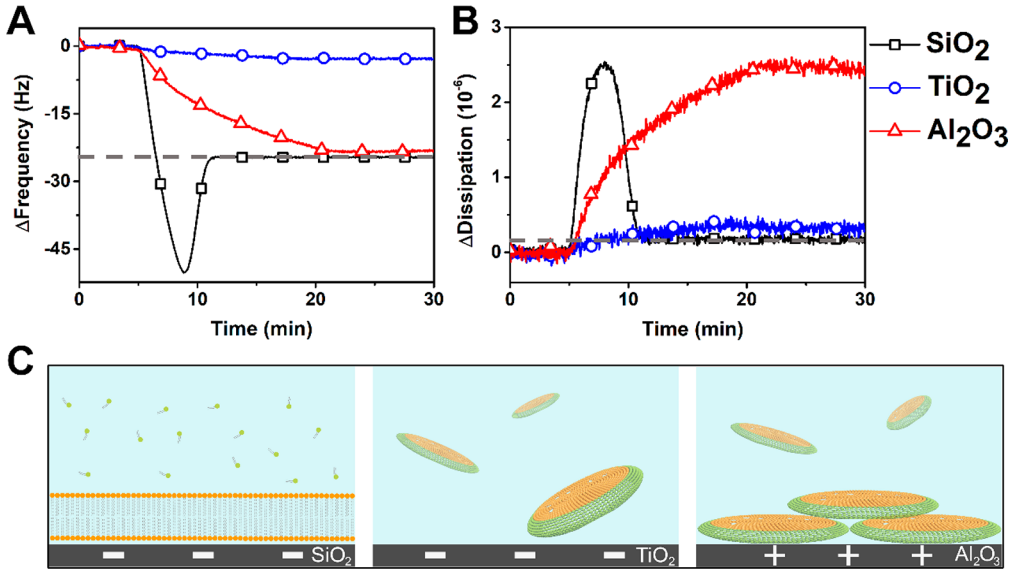

Figure 2. Zwitterionic lipid bicelle adsorption onto various oxide surfaces. Changes in the QCM-D (A) frequency and (B) energy dissipation signals were recorded as a function of time for bicelle adsorption onto silicon dioxide, titanium oxide, and aluminum oxide surfaces. Bicelles were added at t = 5 min. The dotted lines represent typical QCM-D measurement values for an SLB. (C) Schematic illustrations of the experimental results. The illustrations are not drawn to scale.

(DOPS) among the long-chain phospholipids used in the bicelle preparation process along with a fixed amount of 1,2-dihexanoyl-*sn*-glycero-3-phosphocholine (DHPC) short-chain phospholipid—opens the door to modulating bicelle—substrate interactions and gaining fundamental insights into dynamic bicelle adsorption, fusion, and rupture processes. Quartz crystal microbalance-dissipation (QCM-D) measurements were conducted in order to track the corresponding adsorption kinetics and evaluate SLB formation quality. Our findings provide insight into the general utility of the bicelle-mediated SLB formation method on various oxide surfaces while revealing how the presence of charged lipids affects bicelle—substrate interactions and hence influences adsorption pathways. Such information can also help researchers select optimal conditions and lipid compositions for conducting the bicelle-mediated SLB formation method on different surfaces.

MATERIALS AND METHODS

Reagents. 1,2-dioleoyl-*sn*-glycero-3-phosphocholine (DOPC), 1,2-dioleoyl-*sn*-glycero-3-ethylphosphocholine (chloride salt) (DOEPC), 1,2-dioleoyl-*sn*-glycero-3-phospho-L-serine (sodium salt) (DOPS), and 1,2-dihexanoyl-*sn*-glycero-3-phosphocholine (DHPC) lipids dispersed in chloroform were obtained from Avanti Polar Lipids (Alabaster, AL). Aqueous buffer solutions were prepared using Milli-Q-treated water (>18 MΩ·cm) (MilliporeSigma, Burlington, MA).

Bicelle Preparation. Bicellar aggregates were prepared by lipid hydration followed by freeze—thaw-vortexing, as previously described.[19] The as-supplied chloroform solutions of long-chain phospholipids (DOPC, DOEPC, and DOPS) were mixed in a glass vial to achieve the desired molar ratio and then the chloroform solvent was evaporated by air-blowing with nitrogen gas, resulting in a dry lipid film on the walls of a glass vial. The lipid film was then stored overnight in a vacuum desiccator to remove trace residues of chloroform, followed by subsequent hydration in a DHPC-containing aqueous buffer solution comprising 10 mM Tris (pH 7.5) and 150 mM NaCl. The resulting lipid suspension had a long-chain phospholipid concentration of 1 mM and a q-ratio of 0.25. The lipid suspensions were next treated with five cycles of freeze—thaw-vortex cycling that involved the following steps: submersion in liquid nitrogen for 1 min, thawing in a 60 °C water bath for 5 min, and vortexing for 30 s. The resulting suspensions were visually clear at room temperature. Immediately before experiment, an aliquot of the stock lipid suspension was diluted ∼32-fold by using the buffer solution so that the final long-chain phospholipid concentration was 0.031 mM.

Quartz Crystal Microbalance-Dissipation (QCM-D). Bicelle adsorption experiments were conducted using a Q-Sense E4 instrument (Biolin Scientific AB, Stockholm, Sweden). The quartz crystal sensor chips had a fundamental frequency of 5 MHz and the sensor surface had a 50 nm-thick sputter-coated oxide layer, which was comprised of either silicon dioxide, titanium oxide, or aluminum oxide depending on the experiment. For cleaning purposes, the sensor chips were repeatedly washed with ethanol and water, followed by nitrogen gas drying and then treatment in an oxygen plasma chamber (PDC-002, Harrick Plasma, Ithaca, NY) for 1 min. After chamber assembly, a baseline signal in aqueous buffer solution (10 mM Tris [pH 7.5] and 150 mM NaCl) was first established before the bicelle sample in equivalent buffer solution was added. All solutions were added under continuous flow conditions using a peristaltic pump (Reglo Digital, Ismatec, Glattbrugg, Switzerland) and the flow rate was set at 50 μL/min. Measurement data was collected at multiple odd overtones by the Q-Soft software package (Biolin Scientific AB). The reported data were collected at the fifth overtone and normalized according to the overtone number. Data processing was completed using the Q-Tools (Biolin Scientific AB) and OriginPro (OriginLab, Northampton, MA) software programs.

RESULTS

Zwitterionic Lipid Bicelle Adsorption. We employed the quartz crystal microbalance-dissipation (QCM-D) technique in order to study bicelle adsorption onto silicon dioxide, titanium oxide, and aluminum oxide surfaces. The QCM-D technique tracks changes in the resonance frequency (Δf) and energy dissipation (ΔD) of an oscillating, oxide film-coated quartz crystal as a function of time, and the Δf and ΔD shifts relate to the mass and viscoelastic properties of the adsorbed bicelle layer, respectively.[25] In the experiments, a baseline signal in aqueous buffer solution was first acquired before bicelles were added under continuous flow conditions until the measurement signals stabilized. Then, a buffer washing step was

DOI: 10.1021/acs.langmuir.9b00570
Langmuir 2019, 35, 8436−8444

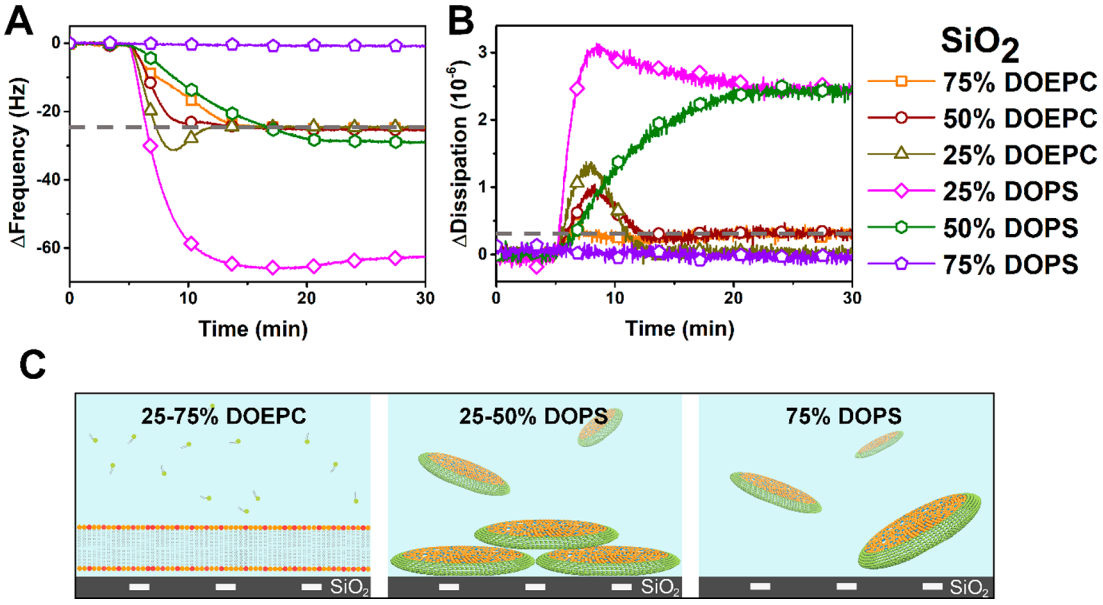

Figure 3. Charged lipid bicelle adsorption onto silicon dioxide surfaces. Changes in the QCM-D (A) frequency and (B) energy dissipation signals were recorded as a function of time for charged lipid bicelle adsorption onto silicon dioxide surfaces. Bicelles were added at t = 5 min. The dotted lines represent typical QCM-D measurement values for an SLB. (C) Schematic illustrations of the experimental results depending on the lipid composition. The illustrations are not drawn to scale.

performed and the final Δf and ΔD shifts were recorded for each measurement run (n = 3 runs per condition). As mentioned above, the long-chain phospholipids used for bicelle preparation were DOPC, DOPS, and DOEPC lipids, and the short-chain phospholipid was DHPC lipid. All three long-chain phospholipids have a dioleoyl chain structure, which is suitable for bicelle preparation.[26,27] Based on the optimal conditions identified in our previous study involving zwitterionic DOPC/DHPC lipid bicelle adsorption onto silicon dioxide surfaces,[19] we defined the following bicelle parameters: q-ratio of 0.25 and long-chain phospholipid concentration of 0.031 mM. The buffer conditions were 10 mM Tris [pH 7.5] and 150 mM NaCl. Silicon dioxide and titanium oxide surfaces have isoelectric points around pH 3.9 ± 0.5 and 2.9 ± 0.1, respectively, and are thus negatively charged under these conditions, whereas aluminum oxide has an isoelectric point around pH 8.7 ± 0.4 and is positively charged.[28]

As a first step, we investigated the adsorption of zwitterionic DOPC/DHPC bicelles onto three oxide surfaces (Figure 2). While PC lipid headgroups are zwitterionic, they are not electrically neutral and instead have a slightly negative surface potential.[29] On silicon dioxide, two-step adsorption kinetics were observed and the final Δf and ΔD shifts were around −25.3 ± 0.9 Hz and 0.1 ± 0.1 × 10^{-6}, respectively. As expected, these values are consistent with SLB formation and the adsorption kinetics are indicative of reaching a critical surface coverage of adsorbed bicelles before SLB formation commences.[30] In marked contrast, bicelle adsorption onto titanium oxide was nearly negligible, with final Δf and ΔD shifts of around −3.2 ± 0.7 Hz and 0.3 ± 0.1 × 10^{-6}, respectively. While zwitterionic lipid vesicles do not rupture on titanium oxide under these solution conditions, they typically adsorb to form a close-packed layer[30] and the present results support that adsorbing zwitterionic lipid bicelles have less favorable lipid−substrate interactions with titanium oxide surfaces than zwitterionic lipid vesicles. This distinction might arise from the larger contact surface area of an adsorbing bicelle disk as compared to a spherical lipid vesicle of equivalent diameter.[31] On the other hand, on aluminum oxide, bicelles exhibited monotonic adsorption, reaching final Δf and ΔD shifts of around −21.4 ± 0.8 Hz and 2.4 ± 0.0 × 10^{-6}, respectively. These values are indicative of bicelle adsorption without SLB formation. As such, the results show that zwitterionic lipid bicelles adsorb and form an SLB on silicon dioxide, do not adsorb on titanium oxide, and adsorb but do not form an SLB on aluminum oxide.

Charged Lipid Bicelle Adsorption. Based on these findings, we next investigated the adsorption of charged lipid bicelles onto the three oxide surfaces. To control membrane surface charge, the long-chain phospholipid composition was composed of positively charged DOEPC/DOPC mixtures or negatively charged DOPS/DOPC mixtures. All bicelle parameters and solution conditions were kept constant as described in the preceding experiments and the QCM-D measurement responses for charged lipid bicelle adsorption on each oxide surface are reported below. The results are discussed in terms of the long-chain phospholipid composition and reported from the most positively charged composition (75/25 mol % DOEPC/DOPC) to the most negatively charged one (75/25 mol % DOPS/DOPC).

Silicon Dioxide. As presented in Figure 3, the adsorption of 75/25 mol % DOEPC/DOPC bicelles led to SLB formation with one-step adsorption kinetics indicating that bicelles ruptured immediately upon adsorption. In this case, the final Δf and ΔD values were around −24.7 ± 0.8 Hz and 0.3 ± 0.2 × 10^{-6}, respectively. Similarly, one-step SLB formation kinetics was observed with 50/50 mol % DOEPC/DOPC bicelles and the final Δf and ΔD values were −25.8 ± 1.0 Hz and 0.3 ± 0.2 × 10^{-6}, respectively. For 25/75 mol % DOEPC/DOPC bicelles, SLB formation still occurred, however, two-step adsorption kinetics indicate that a critical surface coverage of adsorbed bicelles was necessary for SLB formation to occur. The final Δf and ΔD values were around −24.8 ± 0.5 Hz and 0.1 ± 0.2 × 10^{-6}, respectively. As such, highly positively

DOI: 10.1021/acs.langmuir.9b00570
Langmuir 2019, 35, 8436−8444

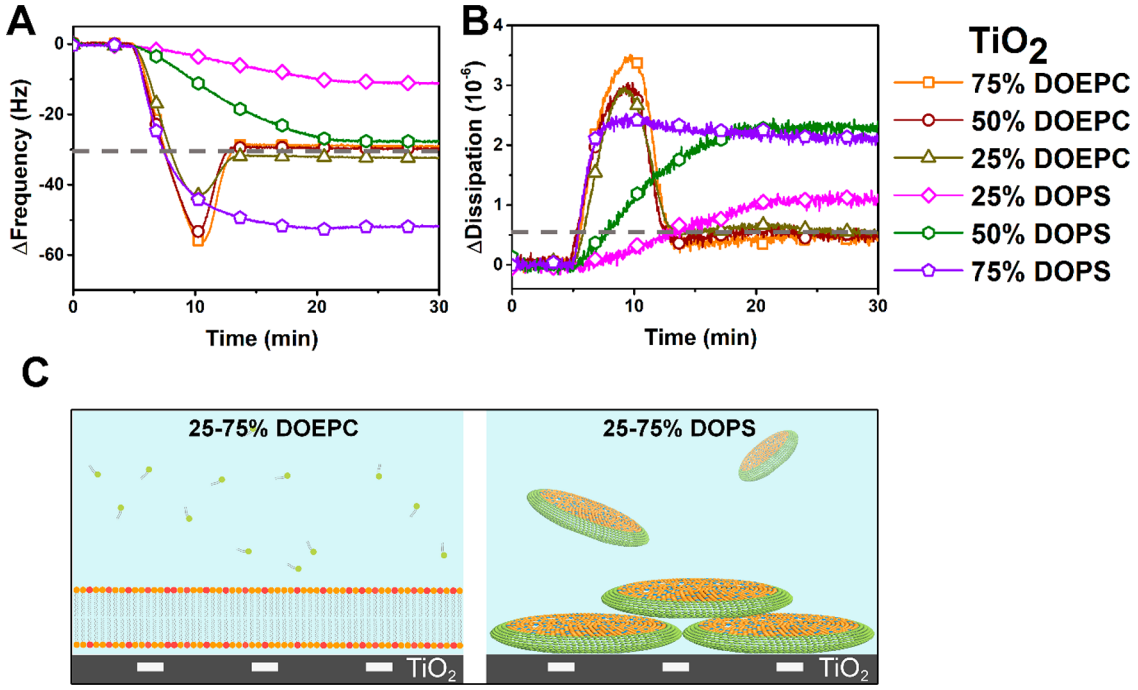

Figure 4. Charged lipid bicelle adsorption onto titanium oxide surfaces. Changes in the QCM-D (A) frequency and (B) energy dissipation signals were recorded as a function of time for charged lipid bicelle adsorption onto titanium oxide surfaces. Bicelles were added at t = 5 min. The dotted lines represent typical QCM-D measurement values for an SLB. (C) Schematic illustrations of the experimental results depending on the lipid composition. The illustrations are not drawn to scale.

charged lipid bicelles rupture immediately upon adsorption, whereas moderately positively charged lipid bicelles behave more like zwitterionic lipid bicelles. Recalling that the silicon dioxide surface is negatively charged under the experimental conditions, these findings point to the importance of electrostatic forces in modulating the strength of bicelle–substrate interactions.

We continued examining the effect of membrane surface charge by investigating the adsorption of negatively charged DOPS/DOPC bicelles. While negative membrane surface charge contributes to electrostatic repulsion between adsorbing bicelles and the silicon dioxide surface, this repulsion is countered by an attractive van der Waals force, and hence, the total interaction energy can be either attractive or repulsive depending on the particular system. The addition of 25/75 mol % DOPS/DOPC bicelles resulted in monotonic adsorption kinetics, with final Δf and ΔD values around -63.1 ± 1.1 Hz and $2.5 \pm 0.3 \times 10^{-6}$, respectively. These values are significantly larger than typical cases for zwitterionic lipid bicelle adsorption, suggesting that a multilayer structure or other type of bicellar aggregate might be contributing to the measurement response in this case. For 50/50 mol % DOPS/DOPC bicelles, monotonic adsorption was also observed although the measurement responses were smaller, with final Δf and ΔD values around -26.5 ± 2.8 Hz and $2.5 \pm 0.2 \times 10^{-6}$, respectively. By contrast, there was only negligible adsorption of 75/25 mol % DOPS/DOPC bicelles, with final Δf and ΔD values of around -2.4 ± 0.4 Hz and $0.1 \pm 0.1 \times 10^{-6}$, respectively. As such, negatively charged lipid bicelles can adsorb onto silicon dioxide surfaces unless the magnitude of electrostatic repulsion is too significant. It should also be pointed out that bicelles, like vesicles and other classes of biological macromolecules, are expected to obey diffusion-limited adsorption kinetics[32] and thus differences in the initial uptake rates are likely related to lipid composition-dependent sizes of the bicellar aggregates in suspension.[33]

Titanium Oxide. As presented in Figure 4, two-step adsorption kinetics and SLB formation occurred with positively charged DOEPC/DOPC lipid bicelles on titanium oxide surfaces. The final Δf and ΔD values were around −29 to −32 Hz and 0.2 to 0.8×10^{-6}, respectively, which are consistent with SLB formation on titanium oxide surfaces.[24] While these values are slightly higher than typical values for SLBs on silica-based surfaces, the difference can be attributed to additional hydrodynamically coupled solvent within the hydration layer separating the SLB from direct contact with the titanium oxide surface.[34] Indeed, it should be noted that the hydration layer on titanium oxide is thicker than that on silicon dioxide due to a stronger van der Waals force.[35,36]

On the other hand, negatively charged bicelles adsorbed onto the titanium oxide surface but did not form SLBs. For 25/75 mol % DOPS/DOPC bicelles, monotonic adsorption occurred with final Δf and ΔD values around -9.3 ± 1.6 Hz and $1.0 \pm 0.1 \times 10^{-6}$, respectively.

Interestingly, the measurement responses became progressively larger with increasing DOPS lipid fraction. For 50/50 mol % DOPS/DOPC bicelles, monotonic adsorption occurred with final Δf and ΔD values around -27.3 ± 0.3 Hz and $2.2 \pm 0.1 \times 10^{-6}$, respectively. Likewise, for 75/25 mol % DOPS/DOPC bicelles, monotonic adsorption occurred with final Δf and ΔD values around -52.4 ± 1.5 Hz and $2.2 \pm 0.2 \times 10^{-6}$, respectively. Taking into account that zwitterionic lipid bicelle adsorption onto titanium oxide is nearly negligible as reported above, the overall trend supports that, with increasing negative membrane surface charge, negatively charged lipid bicelles exhibit more significant adsorption onto titanium oxide surfaces. Since the titanium oxide surface is also negatively charged under the experimental conditions, this result is

DOI: 10.1021/acs.langmuir.9b00570
Langmuir 2019, 35, 8436–8444

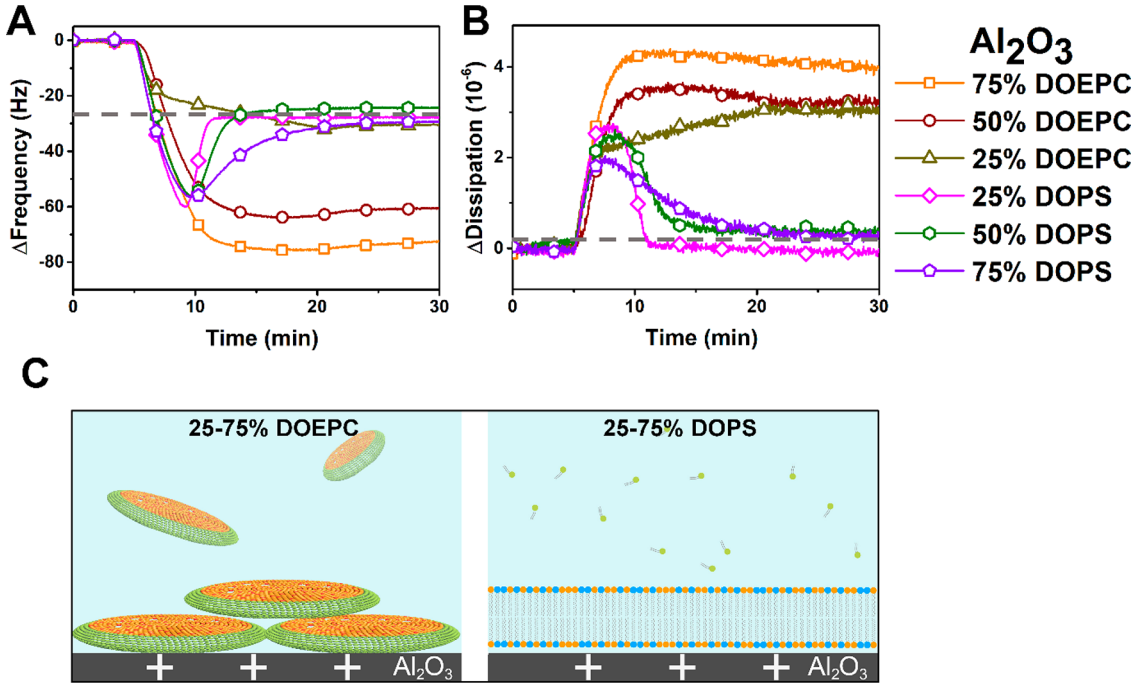

Figure 5. Charged lipid bicelle adsorption onto aluminum oxide surfaces. Changes in the QCM-D (A) frequency and (B) energy dissipation signals were recorded as a function of time for charged lipid bicelle adsorption onto aluminum oxide surfaces. Bicelles were added at t = 5 min. The dotted lines represent typical QCM-D measurement values for an SLB. (C) Schematic illustrations of the experimental results depending on the lipid composition. The illustrations are not drawn to scale.

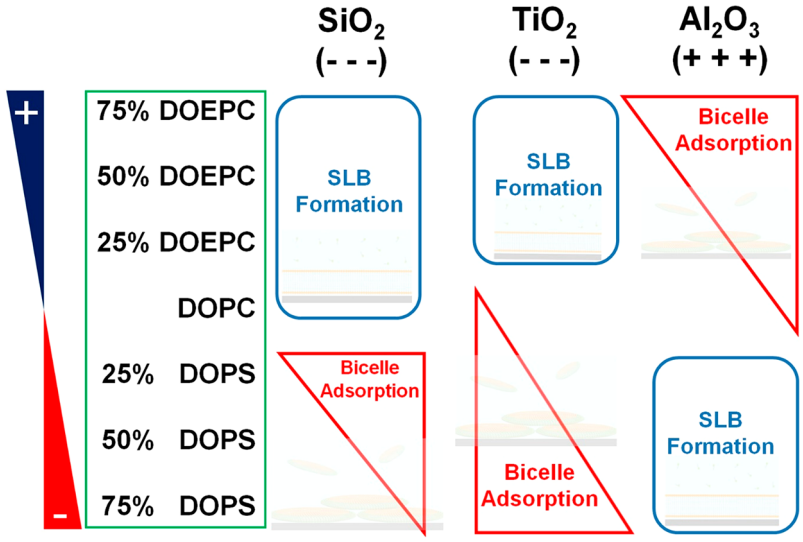

Figure 6. Trends in lipid bicelle adsorption on various oxide surfaces. Depending on the oxide surface, different trends in bicelle−substrate interactions as a function of lipid composition were identified. Bicelle attachment led to SLB formation or monotonic adsorption without SLB formation. The triangle shapes symbolize the relative amount of bicelle adsorption (greater width represents more adsorption and vice versa). The oxide surface-specific variations relate to the surface charge of the substrate material along with other material properties such as material polarizability and the degree of surface hydration.

particularly intriguing because it suggests that the electrostatic force is not the dominant factor influencing the adsorption of negatively charged bicelles onto titanium oxide. Rather, it has been proposed that the hydration force is a key factor,[36] and one possibility in this case is that negatively charged lipid molecules within the adsorbing bicelles affect the ordering of interfacial water molecules within the hydration layer to dissipate the repulsive hydration force. Altogether, the results indicate that positively charged bicelles adsorb and form SLBs on titanium oxide, whereas negatively charged bicelles adsorb but do not form SLBs.

Aluminum Oxide. As presented in Figure 5, there was monotonic adsorption of 75/25 mol % DOEPC/DOPC bicelles onto aluminum oxide surfaces and the final Δf and ΔD values were around -70.2 ± 1.1 Hz and $4.4 \pm 0.8 \times 10^{-6}$, respectively. Similar adsorption kinetics occurred with 50/50 mol % DOEPC/DOPC bicelles and the measurement responses were slightly smaller, with final Δf and ΔD values

DOI: 10.1021/acs.langmuir.9b00570
Langmuir 2019, 35, 8436−8444

around -60.7 ± 0.9 Hz and $3.4 \pm 0.1 \times 10^{-6}$, respectively. For 25/75 mol % DOEPC/DOPC bicelles, monotonic adsorption also occurred and the measurement responses were appreciably smaller, with final Δf and ΔD values around -29.1 ± 1.3 Hz and $3.0 \pm 0.1 \times 10^{-6}$, respectively. Altogether, the trend supports that, with increasing positive membrane surface charge, positively charged lipid bicelles exhibit more significant adsorption onto aluminum oxide surfaces. Since the aluminum oxide surface is positively charged under the experimental conditions, this finding bears a striking resemblance to the case of negatively charged lipid bicelles on negatively charged titanium oxide surfaces. Like titanium oxide, there is a strong hydration force on aluminum oxide surfaces[23] and it is possible in this case that positively charged lipid molecules within the adsorbing bicelles affect the ordering of interfacial water molecules within the hydration layer of the aluminum oxide surface, thereby dissipating the magnitude of the repulsive hydration force and facilitating bicelle adsorption.

By contrast, we identified that negatively charged lipid bicelles exhibited two-step adsorption kinetics, leading to SLB formation on aluminum oxide surfaces. For 25/75 mol % DOPS/DOPC bicelles, the final Δf and ΔD values were around -26.6 ± 1.2 Hz and 0.0×10^{-6}, respectively. Similar responses were recorded for 50/50 mol % DOPS/DOPC bicelles, with final Δf and ΔD values around -25.6 ± 1.6 Hz and $0.1 \pm 0.1 \times 10^{-6}$, respectively. SLB formation also occurred with 75/25 mol % DOPS/DOPC bicelles, and the final Δf and ΔD values were around -29.1 ± 1.1 Hz and $0.2 \pm 0.2 \times 10^{-6}$, respectively. In summary, the results indicate that positively charged bicelles adsorb but do not form SLBs on aluminum oxide, whereas negatively charged bicelles adsorb and form SLBs.

DISCUSSION

Figure 6 summarizes the bicelle adsorption data that were collected on different oxide surfaces, revealing interesting trends on each substrate. Before proceeding to discuss the case of each substrate, we recall that there are principally three interfacial forces that influence lipid–substrate interactions.[36−38] The van der Waals force is an attractive force that is related to material polarizability, whereas the hydration force is a repulsive force that arises from the ordering of interfacial water molecules at a solid–liquid interface. The double-layer electrostatic force can be either attractive or repulsive depending on the surface charges of the two contacting bodies, in our case lipid bicelles and an oxide surface. It has been previously shown that there are particularly strong hydration forces on titanium oxide and aluminum oxide surfaces under the experimental pH conditions,[23,36] which weaken lipid–substrate interactions on these two substrates and help to explain why adsorbed vesicles—another type of lipid nanostructure with high membrane tension—typically do not rupture on them. On the other hand, the magnitude of the hydration force on silicon dioxide surfaces is comparatively low under the experimental pH conditions and hence there are typically stronger lipid–substrate interactions that permit adsorbed vesicles to rupture, whereas other interfacial forces appear to play a more influential role in controlling adsorption pathways on silicon dioxide.

With these points in mind, we turn our attention to the silicon dioxide data. One-step SLB formation was observed for highly positively charged lipid bicelles, whereas two-step SLB formation occurred for moderately positively charged lipid bicelles and zwitterionic lipid bicelles. On the other hand, negatively charged lipid bicelles exhibited monotonic adsorption, and the adsorption uptake decreased with increasingly negative membrane surface charge. Greater electrostatic attraction led to stronger bicelle–substrate interactions, whereas greater electrostatic repulsion contributed to weaker bicelle–substrate interactions. All of these findings are consistent with electrostatic forces playing a key role in modulating lipid adsorption pathways on silicon dioxide surfaces.[37,39]

The titanium oxide and aluminum oxide data sets reveal trends in adsorption pathways that are distinct from the silicon dioxide case and warrant closer attention. On titanium oxide, SLB formation occurs for positively charged lipid bicelles, which is consistent with strong electrostatic attraction with the negatively charged titanium oxide surface. However, negligible adsorption is observed for zwitterionic lipid bicelles and negatively charged lipid bicelles adsorb but do not rupture. One particularly interesting aspect is that, with greater negative membrane surface charge, there is more adsorption uptake onto the negatively charged titanium oxide surface. At first glance, the latter observation is seemingly counterintuitive. How can greater bicelle adsorption occur as electrostatic repulsion increases? The exact same pattern in adsorption pathways is observed on aluminum oxide, although the trend is reversed because the aluminum oxide surface is positively charged. Negatively charged lipid bicelles form SLBs on aluminum oxide, while zwitterionic lipid bicelles adsorb to the lowest extent and the adsorption uptake of positively charged lipid bicelles increases with greater positive membrane surface charge.

To explain the trends involving negatively charged lipid bicelles on negatively charged titanium oxide and positively charged lipid bicelles on positively charged aluminum oxide, we recall that there is a relatively thick hydration layer of interfacial water molecules on these two oxide surfaces. On both substrates, the interfacial water molecules experience a strong ordering effect due to the negative or positive surface charge of the oxide surface.[40,41] This ordering is what gives rise to steric-hydration repulsion,[38] and disrupting this ordering would consequently decrease the magnitude of the hydration force.[42−44] As such, when a charged lipid bicelle with equivalent charge type adsorbs onto the surface, the ordered water molecules may become disoriented due to the competing influences of the surface potentials of the bicelle and oxide substrate. For example, water molecules are aligned according to the negative surface charge of a titanium oxide surface,[41] however, the presence of negatively charged lipid headgroups in close proximity would likely cause the water molecules to attempt to "flip-flop" in order to align themselves with the lipid molecules. Such competing factors could attenuate the magnitude of the hydration force and this picture is consistent with the experimental data, as well as with past experimental reports on protein adsorption.[45] It is also revealing that such trends are observed on both titanium oxide and aluminum oxide—two substrates that are known to have strong hydration forces—but not on silicon dioxide, which is known to have a relatively weaker hydration force under the experimental conditions. As such, the experimental trends are consistent with electrostatic forces playing a key role to promote SLB formation and dictate bicelle adsorption pathways on silicon dioxide, whereas hydration forces help to explain the

DOI: 10.1021/acs.langmuir.9b00570
Langmuir 2019, 35, 8436−8444

interesting trends observed for intact bicelle adsorption on titanium oxide and aluminum oxide surfaces.

CONCLUSION

In summary, our findings demonstrate that lipid bicelles exhibit distinct adsorption behaviors on silicon dioxide, titanium oxide, and aluminum oxide surfaces. The adsorption pathways can be classified into three categories: (i) SLB formation via one- or two-step adsorption kinetics, (ii) monotonic adsorption without SLB formation, and (iii) negligible adsorption. Interestingly, on all three substrates, it was possible to fabricate SLBs; however, the specific lipid compositions varied in each case. On silicon dioxide, positively charged and zwitterionic lipid bicelles formed SLBs. On titanium oxide, positively charged lipid bicelles formed SLBs, whereas negatively charged lipid bicelles formed SLBs on aluminum oxide. The experimental data indicate that electrostatic attraction between the oxide surface and adsorbing bicelles is necessary for successful SLB formation. In the case of bicelle adsorption alone, the results also show that there are clear differences between oxide surfaces with low surface hydration (i.e., silicon dioxide) and oxide surfaces with high surface hydration (i.e., titanium oxide and aluminum oxide). These trends can be understood in terms of the relative contributions of different interfacial forces, namely double-layer electrostatic and hydration forces, to modulating bicelle−substrate interactions. Altogether, the findings in this work establish a roadmap to utilize bicellar mixtures to form SLBs on hydrophilic surfaces with different material properties, and also provide insight into the physicochemical factors that influence bicelle−substrate interactions.

AUTHOR INFORMATION

Corresponding Author

*E-mail: njcho@ntu.edu.sg.

ORCID

Joshua A. Jackman: 0000-0002-1800-8102

Nam-Joon Cho: 0000-0002-8692-8955

Notes

The authors declare no competing financial interest.

ACKNOWLEDGMENTS

This work was supported by the National Research Foundation of Singapore through a Competitive Research Programme grant (NRF-CRP10-2012-07) and a Proof-of-Concept grant (NRF2015NRF-POC0001-19) as well as through the Center for Precision Biology at Nanyang Technological University. Additional support was provided by the Creative Materials Discovery Program through the National Research Foundation of Korea funded by the Ministry of Science, ICT and Future Planning (NRF-2016M3D1A1024098).

REFERENCES

(1) Ariga, K.; Leong, D. T.; Mori, T. Nanoarchitectonics for Hybrid and Related Materials for Bio-Oriented Applications. *Adv. Funct. Mater.* **2018**, *28* (27), 1702905.

(2) Ariga, K.; Watanabe, S.; Mori, T.; Takeya, J. Soft 2D Nanoarchitectonics. *NPG Asia Mater.* **2018**, *10*, 1.

(3) Bally, M.; Bailey, K.; Sugihara, K.; Grieshaber, D.; Vörös, J.; Städler, B. Liposome and Lipid Bilayer Arrays Towards Biosensing Applications. *Small* **2010**, *6* (22), 2481−2497.

(4) Mazur, F.; Bally, M.; Städler, B.; Chandrawati, R. Liposomes and Lipid Bilayers in Biosensors. *Adv. Colloid Interface Sci.* **2017**, *249*, 88−99.

(5) Komiyama, M.; Yoshimoto, K.; Sisido, M.; Ariga, K. Chemistry Can Make Strict and Fuzzy Controls for Bio-Systems: DNA Nanoarchitectonics and Cell-Macromolecular Nanoarchitectonics. *Bull. Chem. Soc. Jpn.* **2017**, *90* (9), 967−1004.

(6) Ram, P.; Prestegard, J. Magnetic Field Induced Ordering of Bile Salt/Phospholipid Micelles: New Media for NMR Structural Investigations. *Biochim. Biophys. Acta, Biomembr.* **1988**, *940* (2), 289−294.

(7) Marcotte, I.; Auger, M. Bicelles as Model Membranes for Solid- and Solution-State NMR Studies of Membrane Peptides and Proteins. *Concepts Magn. Reson., Part A* **2005**, *24* (1), 17−37.

(8) Glover, K. J.; Whiles, J. A.; Wu, G.; Yu, N.-j.; Deems, R.; Struppe, J. O.; Stark, R. E.; Komives, E. A.; Vold, R. R. Structural Evaluation of Phospholipid Bicelles for Solution-State Studies of Membrane-Associated Biomolecules. *Biophys. J.* **2001**, *81* (4), 2163−2171.

(9) van Dam, L.; Karlsson, G.; Edwards, K. Direct Observation and Characterization of DMPC/DHPC Aggregates under Conditions Relevant for Biological Solution NMR. *Biochim. Biophys. Acta, Biomembr.* **2004**, *1664* (2), 241−256.

(10) Nieh, M.-P.; Raghunathan, V.; Glinka, C. J.; Harroun, T. A.; Pabst, G.; Katsaras, J. Magnetically Alignable Phase of Phospholipid "Bicelle" Mixtures Is a Chiral Nematic Made up of Wormlike Micelles. *Langmuir* **2004**, *20* (19), 7893−7897.

(11) Triba, M. N.; Devaux, P. F.; Warschawski, D. E. Effects of Lipid Chain Length and Unsaturation on Bicelles Stability. A Phosphorus NMR Study. *Biophys. J.* **2006**, *91* (4), 1357−1367.

(12) De Angelis, A. A.; Opella, S. J. Bicelle Samples for Solid-State NMR of Membrane Proteins. *Nat. Protoc.* **2007**, *2* (10), 2332.

(13) Dürr, U. H.; Gildenberg, M.; Ramamoorthy, A. The Magic of Bicelles Lights up Membrane Protein Structure. *Chem. Rev.* **2012**, *112* (11), 6054−6074.

(14) Castellana, E. T.; Cremer, P. S. Solid Supported Lipid Bilayers: From Biophysical Studies to Sensor Design. *Surf. Sci. Rep.* **2006**, *61* (10), 429−444.

(15) Hardy, G. J.; Nayak, R.; Zauscher, S. Model Cell Membranes: Techniques to Form Complex Biomimetic Supported Lipid Bilayers Via Vesicle Fusion. *Curr. Opin. Colloid Interface Sci.* **2013**, *18* (5), 448−458.

(16) Zeineldin, R.; Last, J. A.; Slade, A. L.; Ista, L. K.; Bisong, P.; O'Brien, M. J.; Brueck, S.; Sasaki, D. Y.; Lopez, G. P. Using Bicellar Mixtures to Form Supported and Suspended Lipid Bilayers on Silicon Chips. *Langmuir* **2006**, *22* (19), 8163−8168.

(17) Tabaei, S. R.; Jönsson, P.; Brändén, M.; Höök, F. Self-Assembly Formation of Multiple DNA-Tethered Lipid Bilayers. *J. Struct. Biol.* **2009**, *168* (1), 200−206.

(18) Morigaki, K.; Kimura, S.; Okada, K.; Kawasaki, T.; Kawasaki, K. Formation of Substrate-Supported Membranes from Mixtures of Long-and Short-Chain Phospholipids. *Langmuir* **2012**, *28* (25), 9649−9655.

(19) Kolahdouzan, K.; Jackman, J. A.; Yoon, B. K.; Kim, M. C.; Johal, M. S.; Cho, N.-J. Optimizing the Formation of Supported Lipid Bilayers from Bicellar Mixtures. *Langmuir* **2017**, *33* (20), 5052−5064.

(20) Mapar, M.; Jõemetsa, S.; Pace, H.; Zhdanov, V. P.; Agnarsson, B. r.; Höök, F. Spatiotemporal Kinetics of Supported Lipid Bilayer Formation on Glass Via Vesicle Adsorption and Rupture. *J. Phys. Chem. Lett.* **2018**, *9* (17), 5143−5149.

(21) Saleem, Q.; Zhang, Z.; Petretic, A.; Gradinaru, C. C.; Macdonald, P. M. Single Lipid Bilayer Deposition on Polymer Surfaces Using Bicelles. *Biomacromolecules* **2015**, *16* (3), 1032−1039.

(22) Yamada, N. L.; Sferrazza, M.; Fujinami, S. In-Situ Measurement of Phospholipid Nanodisk Adhesion on a Solid Substrate Using Neutron Reflectometry and Atomic Force Microscopy. *Phys. B* **2018**, *551*, 222−226.

(23) Jackman, J. A.; Tabaei, S. R.; Zhao, Z.; Yorulmaz, S.; Cho, N.-J. Self-Assembly Formation of Lipid Bilayer Coatings on Bare

DOI: 10.1021/acs.langmuir.9b00570
Langmuir 2019, 35, 8436−8444

Aluminum Oxide: Overcoming the Force of Interfacial Water. *ACS Appl. Mater. Interfaces* **2015**, *7* (1), 959−968.
(24) Tabaei, S. R.; Jackman, J. A.; Kim, S.-O.; Zhdanov, V. P.; Cho, N.-J. Solvent-Assisted Lipid Self-Assembly at Hydrophilic Surfaces: Factors Influencing the Formation of Supported Membranes. *Langmuir* **2015**, *31* (10), 3125−3134.
(25) Cho, N.-J.; Frank, C. W.; Kasemo, B.; Höök, F. Quartz Crystal Microbalance with Dissipation Monitoring of Supported Lipid Bilayers on Various Substrates. *Nat. Protoc.* **2010**, *5* (6), 1096.
(26) Morrison, E. A.; Henzler-Wildman, K. A. Reconstitution of Integral Membrane Proteins into Isotropic Bicelles with Improved Sample Stability and Expanded Lipid Composition Profile. *Biochim. Biophys. Acta, Biomembr.* **2012**, *1818* (3), 814−820.
(27) Rodríguez, G.; Rubio, L.; Barba, C.; López-Iglesias, C.; de la Maza, A.; López, O.; Cócera, M. Characterization of New DOPC/DHPC Platform for Dermal Applications. *Eur. Biophys. J.* **2013**, *42* (5), 333−345.
(28) Cuddy, M. F.; Poda, A. R.; Brantley, L. N. Determination of Isoelectric Points and the Role of pH for Common Quartz Crystal Microbalance Sensors. *ACS Appl. Mater. Interfaces* **2013**, *5* (9), 3514−3518.
(29) Yang, Y.; Mayer, K. M.; Hafner, J. H. Quantitative Membrane Electrostatics with the Atomic Force Microscope. *Biophys. J.* **2007**, *92* (6), 1966−1974.
(30) Keller, C.; Kasemo, B. Surface Specific Kinetics of Lipid Vesicle Adsorption Measured with a Quartz Crystal Microbalance. *Biophys. J.* **1998**, *75* (3), 1397−1402.
(31) Zhdanov, V.; Kasemo, B. Comments on Rupture of Adsorbed Vesicles. *Langmuir* **2001**, *17* (12), 3518−3521.
(32) Zhdanov, V.; Keller, C.; Glasmästar, K.; Kasemo, B. Simulation of Adsorption Kinetics of Lipid Vesicles. *J. Chem. Phys.* **2000**, *112* (2), 900−909.
(33) Kot, E. F.; Arseniev, A. S.; Mineev, K. S. Behavior of Most Widely Spread Lipids in Isotropic Bicelles. *Langmuir* **2018**, *34* (28), 8302−8313.
(34) Ferhan, A. R.; Spackova, B.; Jackman, J. A.; Ma, G. J.; Sut, T. N.; Homola, J.; Cho, N.-J. Nanoplasmonic Ruler for Measuring Separation Distance between Supported Lipid Bilayers and Oxide Surfaces. *Anal. Chem.* **2018**, *90* (21), 12503−12511.
(35) Reimhult, E.; Höök, F.; Kasemo, B. Intact Vesicle Adsorption and Supported Biomembrane Formation from Vesicles in Solution: Influence of Surface Chemistry, Vesicle Size, Temperature, and Osmotic Pressure. *Langmuir* **2003**, *19* (5), 1681−1691.
(36) Jackman, J. A.; Zan, G. H.; Zhao, Z.; Cho, N.-J. Contribution of the Hydration Force to Vesicle Adhesion on Titanium Oxide. *Langmuir* **2014**, *30* (19), 5368−5372.
(37) Cremer, P. S.; Boxer, S. G. Formation and Spreading of Lipid Bilayers on Planar Glass Supports. *J. Phys. Chem. B* **1999**, *103* (13), 2554−2559.
(38) Tero, R.; Ujihara, T.; Urisu, T. Lipid Bilayer Membrane with Atomic Step Structure: Supported Bilayer on a Step-and-Terrace TiO_2 (100) Surface. *Langmuir* **2008**, *24* (20), 11567−11576.
(39) Biswas, K. H.; Jackman, J. A.; Park, J. H.; Groves, J. T.; Cho, N.-J. Interfacial Forces Dictate the Pathway of Phospholipid Vesicle Adsorption onto Silicon Dioxide Surfaces. *Langmuir* **2018**, *34* (4), 1775−1782.
(40) Kim, J.; Kim, G.; Cremer, P. S. Investigations of Water Structure at the Solid/Liquid Interface in the Presence of Supported Lipid Bilayers by Vibrational Sum Frequency Spectroscopy. *Langmuir* **2001**, *17* (23), 7255−7260.
(41) Kataoka, S.; Gurau, M. C.; Albertorio, F.; Holden, M. A.; Lim, S.-M.; Yang, R. D.; Cremer, P. S. Investigation of Water Structure at the TiO_2/Aqueous Interface. *Langmuir* **2004**, *20* (5), 1662−1666.
(42) Tero, R.; Watanabe, H.; Urisu, T. Supported Phospholipid Bilayer Formation on Hydrophilicity-Controlled Silicon Dioxide Surfaces. *Phys. Chem. Chem. Phys.* **2006**, *8* (33), 3885−3894.
(43) Ahmed, S.; Madathingal, R. R.; Wunder, S. L.; Chen, Y.; Bothun, G. Hydration Repulsion Effects on the Formation of Supported Lipid Bilayers. *Soft Matter* **2011**, *7* (5), 1936−1947.
(44) Tero, R. Substrate Effects on the Formation Process, Structure and Physicochemical Properties of Supported Lipid Bilayers. *Materials* **2012**, *5* (12), 2658−2680.
(45) Kim, J.; Cremer, P. S. Elucidating Changes in Interfacial Water Structure Upon Protein Adsorption. *ChemPhysChem* **2001**, *2* (8−9), 543−546.

DOI: 10.1021/acs.langmuir.9b00570
Langmuir 2019, 35, 8436−8444